Thermodynamics and multicorrelations of intermittent dynamics

Tatsuharu Kobayashi,* Hirokazu Fujisaka, and Wolfram Just†
Department of Physics, Kyushu University 33, Fukuoka 812, Japan
(Received 6 October 1992)

Statistical properties of type-I intermittency are investigated from the standpoint of the long-time description and time correlations of intermittent time series by utilizing the So-Ose-Mori mapping. It is shown that the two coexisting characteristics, laminar state and burst, can be singled out in a clear-cut way by introducing the ensemble processing with a parameter q. For $q \to -\infty$, the relevant statistical quantities describe the statistics of a purely laminar state and, for $q \to \infty$, they describe the statistics of a purely burst behavior. In particular the dynamical statistical characteristics (temporal correlations) turn out to exhibit clear-cut change at the so-called q-phase transition point q_c in the limit of the intermittency transition of the control parameter. For $q < q_c$, the spectral density takes a power-law form of the frequency, the exponent 2 being independent of q. On the other hand, for $q > q_c$ it has a white-noise spectrum. These are characteristics of the pure laminar state and burst, respectively.

PACS number(s): 02.50.−r, 05.45.+b

I. INTRODUCTION

Chaos showed that even though a dynamical law is simple, it can exhibit complex behavior [1]. This is due to the existence of intrinsic trajectory instability of the dynamical system. Thus we find ourselves unable to understand the complex system in a predictable way, even though the law of evolution is completely known. For this reason, it is necessary to describe such chaotic systems in a statistical manner. For a Gaussian stochastic variable, observing quantities such as the average or the variance is sufficient for an overall description. However, these quantities are too approximate to explain the complex behavior that is generated by deterministic chaos which consists of large fluctuations around the average. These are due to the wandering of the phase point over all unstable periodic orbits. Therefore we introduce the idea of capturing all invariant sets in the system. In Ref. [2], we proposed one approach to analyze the system fluctuation by introducing the parameter q which changes the weight realization of probability (q-weighted average). Roughly speaking, each q corresponds to one invariant measure. A similar idea is also used in fractal objects [3].

The fundamental idea of both the so-called $f(\alpha)$ spectrum [3] and the q-weighted average is that one can single out any characteristic of invariant set by changing the value of q, the degree of weighting. If one makes q correspond to the inverse temperature in statistical mechanics, these formalisms also correspond to the thermodynamics. Hence these are called thermodynamic formalism [2–6]. This formalism of dynamical system has been discussed traditionally from the view of the ergodic theory in mathematics literature [7]. A similar formalism has been found in the probability theory, namely the large deviation theory [8].

The type-I intermittency is one typical route to the onset of chaos, observed in the broad fields such as chemical reactions, fluid systems, magnetic systems, and so on [1]. The intermittent chaos has two characteristic regions: one is the laminar region where the system behaves regularly, and the other is the burst region where the strong trajectory instability exists, yielding the random reinjection. As the control parameter is changed, the phase point suddenly starts to wander these regions.

The purpose of the present paper is to investigate the statistical properties of the type-I intermittent chaos by making use of the q-weighted average of the relevant quantities and the order-q power spectrum. The latter is introduced in order to study the various aspects of time correlations (multicorrelations) corresponding to many invariant measures. We will give a brief review of the general aspects of the present approach to q-weighted average and the order-q power spectrum in Sec. II. In Sec. III the model with Markov partitions is given. We take the So-Ose-Mori (SOM) map [9], which consists of three linear parts as shown in Fig. 1(a). The general analysis method for the Markov partition is also presented. In Sec. IV we study the dynamics of the symbolized coordinate (SC), and obtain some exact results for the q-weighted average as well as the order-q power spectrum. Section V is devoted to the numerical analysis of the dynamics of local expansion rate (LER). Some conclusions are given in Sec. VI.

II. FORMULATION FOR DYNAMICAL FLUCTUATION

We describe here briefly the method of extracting long-time statistical characteristics and multicorrelations for dynamical fluctuations. Let us consider a steady, stochastic time series $\{u_j\}$ $(j=1,2,3,\ldots)$ numerically or experimentally observed. The finite-span average defined by

$$\overline{U}_n = \frac{1}{n} \sum_{j=1}^{n} u_j \tag{2.1}$$

takes various values depending on the span length n over which the average is taken. This approaches the ensem-

ble average $\bar{U}_\infty$, which takes a unique value, and is identical to the ensemble average $\langle u \rangle$ under the ergodicity assumption. The probability density $P_n(U')$ that $\bar{U}_n$ takes the value U' is given by

$$P_n(U')=\langle \delta(\bar{U}_n-U') \rangle , \tag{2.2}$$

where $\delta(g)$ is the delta function of g and $\langle\ \rangle$ denotes the average over the natural invariant measure which is made of the histogram for values of $\bar{U}_n$ from $\{u_j\}$ or is practically equal to the time average under the Sinai-Ruelle-Bowen (SRB) property. Let us introduce the fluctuation spectrum of $\sigma(U)$ by

$$\sigma(U)=-\lim_{n\to\infty}\frac{1}{n}\ln P_n(U) . \tag{2.3}$$

This function evaluates the overall shape of the probability density $P_n(U)$ and is relevant to how the probability for the fluctuation with the value $U(\neq\bar{U}_\infty)$ decreases, as n is increased. The fluctuation spectrum $\sigma(U)$ plays a fundamental role for the long-time (overall) characterizations of the time series $\{u_j\}$. Moreover, let us introduce the characteristic function $\phi(q)$ defined by

$$\phi(q)=\lim_{n\to\infty}\frac{1}{n}\ln M_q(n) , \tag{2.4a}$$

where the generating function $M_q(n)$ is given by

$$M_q(n)=\langle e^{nq\bar{U}_n} \rangle . \tag{2.4b}$$

Substituting the asymptotic form $P_n(U)\sim e^{-n\sigma(U)}$ into (2.4b), we obtain

$$\phi(q)=-\min_{U'}[\sigma(U')-qU'] , \tag{2.5}$$

where the use of the saddle-point evaluation was made, assuming the concavity of σ [$\sigma''(U)>0$]. We define

$$U(q)=\frac{d\phi(q)}{dq} , \tag{2.6a}$$

$$\chi(q)\equiv\lim_{n\to\infty} n\langle[\bar{U}_n-U(q)]^2 e^{nq\bar{U}_n}\rangle/M_q(n)=\frac{dU(q)}{dq} , \tag{2.6b}$$

where $U(q)$ and $\chi(q)$ are, respectively, the average and the variance with respect to the SRB measure (in case of changing the weight of probability through q). The variance $\chi(q)$ turns out to be identical to the derivative of the weighted average $U(q)$ with respect to q. The functions $\sigma(U)$ and $\phi(q)$ are related to each other via the Legendre transform

$$\sigma(U)=qU-\phi(q),\quad q=\frac{d\sigma(U)}{dU} . \tag{2.7}$$

These are fundamental functions for finding hidden fluctuations, but yield no explicit information on temporal correlations. We call them static fluctuation functions. Some functions which are equivalent to fluctuation functions are discussed broadly in Refs. [6,10].

In order to extract dynamical correlations, we define the order-q power spectrum $I_q(\omega)$ by

$$I_q(\omega)=\lim_{n\to\infty}\frac{\langle F_n(\omega,q)\delta(\bar{U}_n-U(q))\rangle}{P_n(U(q))} , \tag{2.8}$$

where

$$F_n(\omega,q)=\left|\frac{1}{\sqrt{n}}\sum_{j=0}^{n-1}\hat{u}_j e^{-i\omega j}\right|^2,\quad \hat{u}_j\equiv u_j-U(q)$$

is the power spectral density of Fourier modes. $I_q(\omega)$ is equivalent to the power spectrum of $\{u_j\}$ over time regions where the averages $\bar{U}_n$ take the same value $U(q)$. In this sense $I_q(\omega)$ describes the specific temporal correlation over the time region whose average of $\{u_j\}$ takes the value $U(q)$. One should note that the average (2.8) can be written in a different way as

$$I_q(\omega)=\lim_{n\to\infty}\frac{\langle F_n(\omega,q)e^{qn\bar{U}_n}\rangle}{M_q(n)} . \tag{2.9}$$

For $q=0$, $I_q(\omega)$ coincides with the ordinary power spectrum. As the span length is long enough, the average value can be uniquely determined for almost all initial conditions. In other words, the large fluctuation due to unstable periodic cycles cannot be observed under natural measure whereas $I_q(\omega)$ is able to capture such a time correlation [11].

In a similar way to $I_q(\omega)$, we introduce the order-q double time correlation function $C_q(t)$ by

$$C_q(t)=\lim_{j\to\infty}\lim_{n\to\infty}\langle\hat{u}_j\hat{u}_{j+t}\delta(\bar{U}_n-U(q))\rangle/P_n(U(q)) \tag{2.10a}$$

$$=\lim_{j\to\infty}\lim_{n\to\infty}\langle\hat{u}_j\hat{u}_{j+t}e^{nq\bar{U}_n}\rangle/M_q(n) . \tag{2.10b}$$

$C_q(t)$ and $I_q(\omega)$ are related to each other via the Wiener-Khinchin theorem:

$$C_q(t)=\frac{1}{2\pi}\int_{-\infty}^{\infty}I_q(\omega)e^{-i\omega t}d\omega , \tag{2.11a}$$

$$I_q(j)=\sum_{t=-\infty}^{\infty}C_q(t)e^{i\omega t} . \tag{2.11b}$$

Thus we can get $C_q(t)$ from $I_q(\omega)$ [11]. One should mentioned that the equality

$$\lim_{\omega\to0}I_q(\omega)=\chi(q)=\sum_{t=-\infty}^{\infty}C_q(t) \tag{2.12}$$

holds.

We call (2.8) and (2.9), respectively, the microcanonical average and the canonical average. The latter is useful to calculate $I_q(\omega)$ from time series.

In the case of one-dimensional chaotic map $x_{n+1}=f(x_n)$, fluctuation functions can be expanded by using the generalized Frobenius-Perron (GFP) operator H_q as follows [12]. Let us define the GFP operator H_q as

$$H_qG(x)=\int e^{qu(y)}\delta(x-f(y))G(y)dy \tag{2.13}$$

for any function $G(x)$, where u_j is assumed to be generated via $u_j=u(x_j)$, $u(x)$ being a unique function of x. With the help of the GFP operator, $M_q(n)$ is rewritten in

the following way:

$$M_q(n)=\int H_q^n \rho(x)dx \ , \tag{2.14}$$

where $\rho(x)$ is the natural invariant density, and satisfies $\rho(x)=H\rho(x)$, H being the ordinary Frobenius-Perron operator ($H=H_{q=0}$). Let ν_q be the largest eigenvalue of H_q. The Perron-Frobenius theorem says ν_q is always positive. The asymptotic form $M_q(n)\sim[\nu_q]^n$ for large n thus yields

$$\phi(q)=\ln\nu_q \ . \tag{2.15}$$

To get the static fluctuation functions $\phi(q),U(q),\chi(q)$, and $\sigma(U)$ therefore we need only the largest eigenvalue of H_q.

On the other hand, as shown in Ref. [13], the order-q power spectrum is expanded as

$$I_q(\omega)=\int v^{(0)}(x)\hat{u}(x)[J_q(\omega)+J_q(-\omega) -1]\hat{u}(x)h^{(0)}(x)dx \ , \tag{2.16}$$

where $\hat{u}(x)=u(x)-U(q)$ ans

$$J_q(\omega)=\frac{1}{1-\frac{e^{i\omega}}{\nu_q}H_q} \ . \tag{2.17}$$

$v^{(0)}(x)$ and $h^{(0)}(x)$ are left and right eigenfunctions for the largest eigenvalue of H_q, respectively [13]. As shown in Ref. [13] (2.10b) can also be written in terms of H_q in the following way:

$$C_q(t)=\int v^{(0)}(x)\hat{u}(x)\left[\frac{H_q}{\nu_q}\right]^t \hat{u}(x)h^{(0)}(x)dx \ . \tag{2.18}$$

If there exist discrete eigenvalues only, as shown in Ref. [11], then (2.9) can be expanded as

$$I_q(\omega)=\tfrac{1}{2}\sum_i K_q^{(l)}\frac{\sinh[\gamma_q^{(l)}+i\omega_q^{(l)}]}{\sinh^2\left[\frac{\gamma_q^{(l)}+i\omega_q^{(l)}}{2}\right]+\sin^2\left[\frac{\omega}{2}\right]} \ , \tag{2.19}$$

where $\sum_l$ is the summation over all eigenstates and $\nu_q^{(l)}$'s are the eigenvalues of H_q which are ordered such that $\nu_q>|\nu_q^{(1)}|\geq|\nu_q^{(2)}|\geq\cdots$ and

$$e^{-(\gamma_q^{(l)}+i\omega_q^{(l)})}=\nu_q^{(l)}/\nu_q \ , \tag{2.20}$$

$$K_q^{(l)}=\left[\int v_q^{(0)}(x)\hat{u}(x)h_q^{(l)}(x)dx\right] \times\left[\int v_q^{(l)}(x)\hat{u}(x)h_q^{(0)}(x)dx\right] , \tag{2.21}$$

where $v_q^{(l)}(x)$ and $h_q^{(l)}(x)$ are left and right eigenfunctions for the eigenvalue $\nu_q^{(l)}$ of H_q, respectively [13]. Equation (2.19) implies that $I_q(\omega)$ is the superposition of Lorentzian peaks. Thus one finds

$$C_q(t)=\sum_l K_q^{(l)}\exp[-(\gamma_q^{(l)}+i\omega_q^{(l)})t] \ . \tag{2.22}$$

The band-splitting chaos has discrete eigenvalues and in this case critical behaviors of order-q power spectrum have been previously reported [14].

III. MODEL

Hereafter we consider a one-dimensional piecewise linear map, the SOM map [9], which takes the form $x_{n+1}=f(x_n)$ with

$$f(x)=\begin{cases} ax+0.2 & (0\leq x\leq c) \\ a^{-1}(x-0.8)+1 & (c\leq x\leq 0.8) \\ -b^{-1}(x-1) & (0.8\leq x\leq 1) \ , \end{cases} \tag{3.1}$$

where a, b, and c are constants satisfying $1>a>0.6$, $b=0.2$, and $c\equiv 0.8/(1+a)$. Its graph with a laminar orbit is shown in Fig. 1. This dynamics exhibits chaotic behavior in the interval [0,1] for $a>a_c=0.6$, and undergoes a saddle-node bifurcation at $a=a_c$. The map has an attractive fixed point $x^*=0.2/(1-a)$ for $a<a_c$. This chaotic dynamics has two kinds of clear-cut phases. One is the laminar phase for $0<x<0.8$ where the phase point evolves in time in a rather regular manner. The other is the burst phase for $x>0.8$ and is the origin of irregular temporal evolution.

The SOM map has the Markov partition at the value $a=a_m(m=3,4,\ldots)$ where a_m is the real solution of

$$a^{m+1}+a^m-5a+3=0 \ . \tag{3.2}$$

The critical point a_c is given as $a_c=\lim_{m\to\infty}a_m=\frac{3}{5}$. At $a=a_m$ the partition consists of $N=2m+1$ subintervals. Transition probability among these parts can be obtained in straightforward manner by the dynamics given by (3.1). Near a_c, one obtains $m\simeq\ln(a_m-a_c)/\ln 0.6$ [9].

In general, when the system has a Markov partition, the GFP operator H_q can be treated in the matrix form, and we can straightforwardly apply the method discussed in Sec. II. The matrix element of H_q is obtained as

$$(H_q)_{ij}=\begin{cases} \alpha_j, & i=j+1 \\ \alpha_N, & j=N \\ 0 & \text{otherwise,} \end{cases} \tag{3.3}$$

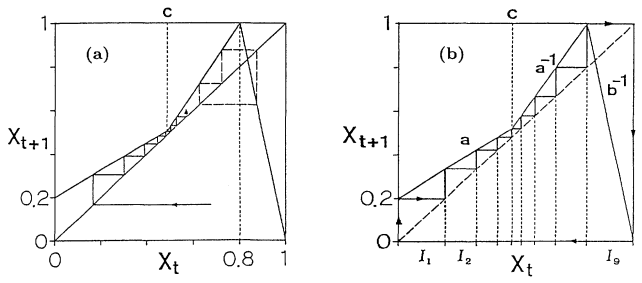

FIG. 1. (a) Graph of the SOM map (3.1) for $a>a_c$, where a laminar orbit (thin solid line) and an unstable periodic orbit with period three (dashed line) are shown. (b) Piecewise linear Markov map with $a=a_4\simeq 0.665$ ($m=4$), where the period-ten orbit (heavy solid line) leads to the Markov partition $\{I_1,I_2,\ldots,I_9\}$.

with

$$\alpha_j = \frac{e^{qv_j}}{|f_i'|} ,$$

where v_j and f_j' are, respectively, the value of $u(x)$ and the slope of $df(x)/dx$ in the jth interval of the partition. In this paper we take $u(x)$ as the (LER) $[u(x)=\ln|f'(x)|]$ and the SC [i.e., $u(x)=1$ for $0.8<x<1$ and 0 otherwise]. Namely v_j takes $\ln|f_j'|$ for LER and $\delta_{i,2m+1}$ for SC, where $\delta_{i,j}$ is Kronecker's delta. The temporal evolutions of these quantities are illustrated in Fig. 2.

Furthermore (2.16) and (2.17) are given by

$$I_q(\omega) = \sum_{\substack{l,m\neq 0 \\ \omega\neq 0}} v_l^{(0)} v_l [J_q(\omega)+J_q(-\omega)-E]_{l,m} v_m h_m^{(0)} , \tag{3.4}$$

$$J_q(\omega) = \frac{1}{E-\frac{e^{i\omega}}{\nu_q}H_q} , \tag{3.5}$$

where E is the $N\times N$ unit matrix and v_l is the value of $\hat{u}(x)$ when x is in the lth interval of the Markov partition. Thus we can get $I_q(\omega)$ from calculations of matrix in the case of Markov partition.

IV. DYNAMICS OF SYMBOLIZED COORDINATE

In this section we will consider the dynamics of the symbolized coordinate and evaluate the fluctuation functions and the order-q power spectra. First we discuss fluctuation functions and q-phase transition. The characteristic equation for the eigenvalue problem is rewritten in the following way:

$$\beta^{-1} = \frac{1-\left[\frac{a}{\nu}\right]^{m+1}}{\nu-a} + \frac{1}{\nu^N}\frac{1-(\nu a)^m}{1-\nu a} , \tag{4.1}$$

where ν is the eigenvalue of the matrix H_q and $\beta=be^q$. One should note that for large m, i.e., near $a=a_c$, all eigenvalues of H_q for $q<q_c$, q_c being a certain value of q as shown later, are located approximately on the unit circle on the complex ν plane. On the other hand, for $q>q_c$ only the largest eigenvalue is isolated and the other remain approximately on the unit circle. By evaluating (4.1) for $m\to\infty$, i.e., in the limit $a\to a_c$, the largest eigenvalue is thus given by

$$\nu_q = \begin{cases} 1 & (q\le q_c) \\ a_c+\beta & (q\ge q_c) , \end{cases} \tag{4.2}$$

where the characteristic value q_c is determined by $\nu_{qc}=1$, which yields $q_c=\ln 2=0.6931\ldots$. Fluctuation functions are calculated easily from (2.4a), (2.6a), and (2.6b), in the limit $a\to a_c$, as

$$\phi(q) = \begin{cases} 0 & \text{for } q\le q_c \\ \ln(a_c+\beta) & \text{for } q\le q_c , \end{cases} \tag{4.3}$$

$$U(q) = \begin{cases} 0 & \text{for } q<q_c \\ \dfrac{\beta}{(a_c+\beta)} & \text{for } q>q_c , \end{cases} \tag{4.4}$$

$$\chi(q) = \begin{cases} 0 & \text{for } q<q_c \\ +\infty & \text{for } q=q_c \\ \dfrac{a_c\beta}{(a_c+\beta)^2} & \text{for } q>q_c . \end{cases} \tag{4.5}$$

The fluctuation spectrum of $\sigma(U)$ is obtained from (2.7) as

$$\sigma(U) = \begin{cases} q_c U & \text{for } 0\le U\le\Delta \\ U\ln\dfrac{U}{b}+(1-U)\ln\dfrac{1-U}{a_c} & \text{for } \Delta\le U\le 1 , \end{cases} \tag{4.6}$$

where $\Delta=U(q_c)=0.4$. Fluctuation functions are drawn in Fig. 3. It turns out that $U(q)$ exhibits a discontinuous transition at $q=q_c$ where $\chi(q_c)$ diverges at $a=a_c+0$. This means that the fluctuation singled out by the parameter value $q=q_c$ becomes extremely large at the transition point $a=a_c$ [see (2.6b)]. Furthermore, the fluctuation spectrum $\sigma(U)$ linearly depends on U in a certain regime of U. Its slope is identical to q_c. We call this anom-

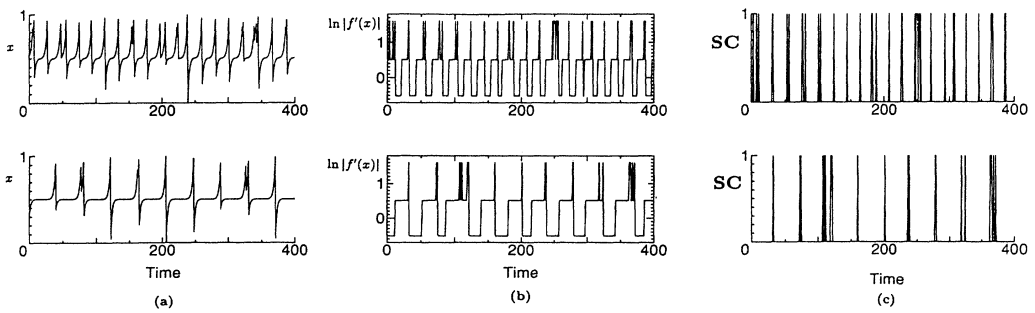

FIG. 2. Time series u_j for SOM map near the onset of chaos (all the upper graphs are for $m=10$ and those below for $m=20$); (a) coordinate x, (b) local expansion rate $\ln|f'(x)|$, (c) symbolized coordinate (1 for $0.8<x<1$ and 0 otherwise). As m gets larger, the intermittency characteristic develops.

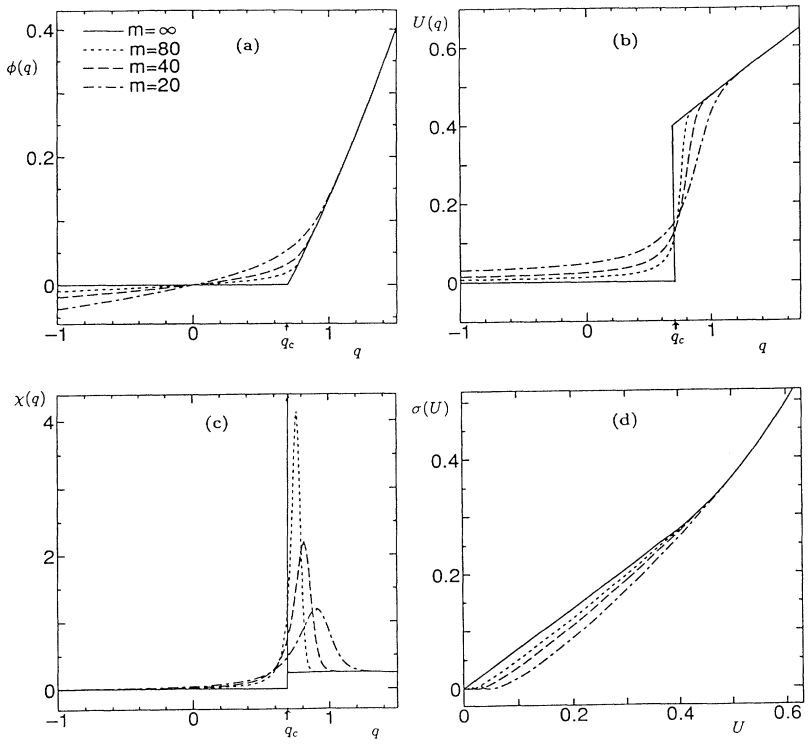

FIG. 3. Static fluctuation functions for SC of the SOM map at the transition point $a=a_c+0$ (solid lines), where $q_c=\ln 2=0.6931\ldots$, $\Delta=U(q_c)=0.4$. The fluctuation functions for finite m, i.e., for finite-number Markov partition, are also drawn.

alous behavior at $q=q_c$ the q-phase transition [10,15]. The fundamental reason for the occurrence of such a transition is due to the enhancement of intermittent behavior, i.e., due to the decrease of the probability that the phase point stays in the burst region. We can thus clearly separate the laminar phase for $q<q_c$ and the burst phase for $q>q_c$. Such separation is possible only by introducing the intensive variable q.

Let $\chi_N(q)$ be the susceptibility calculated with the characteristic function for the periodicity N of the Markov partition $[\chi(q)=\lim_{N\to\infty}\chi_N(q)]$. Evaluating (4.1), we obtain the asymptotic behavior of $\chi_N(q)$. For large N, its peak height $\chi_N(\hat{q})$, where $\hat{q}$ is the peak position of $\chi_N(q)$, obeys

$$\chi_N(\hat{q})\propto N\ . \tag{4.7}$$

Furthermore, the peak position $\hat{q}(N)$ of $\chi_N(q)$ is numerically found to obey

$$q_c-\hat{q}\propto N^{-\eta}\ , \tag{4.8}$$

where $\eta\simeq 0.8$. Thus we observe the phase transition at $q=q_c$ as q is changed near the bifurcation point of chaos. The fluctuation functions for finite N are also drawn in Fig. 3. The above treatment helps us to clearly single out the characteristics of the long-time dynamics composed of laminar and burst phases.

Next we turn to the order-q power spectrum. By taking $u(x)$ as the symbolized coordinate, (3.4) and (3.5) reduce to

$$I_q(\omega)=[J_q(\omega)+J_q(-\omega)-1]\mu_N\ , \tag{4.9}$$

$$J_q(\omega)=\left[\frac{1}{E-\frac{e^{i\omega}}{\nu_q}H_q}\right]_{N,N}\ , \tag{4.10}$$

where μ_N is a normalization constant [13]. Moreover by using (3.3), (4.10) is rewritten in the following way:

$$J_q(\omega)=\frac{1}{1-\beta\left[\dfrac{1-(Da)^{m+1}}{\frac{1}{D}-a}+D^N\dfrac{1-\left[\frac{a}{D}\right]^m}{1-\frac{a}{D}}\right]}\ , \tag{4.11}$$

where $D=e^{i\omega}/\nu_q$. We will discuss the asymptotics of $I_q(\omega)$ for (i) $q>q_c$ and (ii) $q<q_c$ near $a=a_c$.

(i) $q>q_c$ (burst phase). In this region $|D|<1$ so one can neglect all terms with D^m in (4.11) for large m. Thus we obtain

$$J_q(\omega)=\frac{\nu_q-ae^{i\omega}}{\nu_q-(a+\beta)e^{i\omega}}\ . \tag{4.12}$$

Therefore

$$I_q(\omega)=\frac{a}{a+\beta}\mu_N\ . \tag{4.13}$$

$I_q(\omega)$ is thus independent of ω and this implies no temporal correlation, which corresponds to the SOM map containing the structure of the tent map in the burst region.

(ii) $q < q_c$ (laminar phase). In this region the leading term of ν_q is 1, but we must consider the correction of ν_q^{-N}. From (4.1) we obtain

$$\nu_q^{-N} = (1-a-\beta)/\beta \ . \tag{4.14}$$

Inserting (4.14) into (4.11) and replacing ν_q by 1 we obtain

$$J_q(\omega) = \frac{(1-ae^{i\omega})(1-ae^{-i\omega})}{(1-ae^{-i\omega})[1-(a+\beta)e^{i\omega}]-(1-a-\beta)(1-ae^{i\omega})e^{iN\omega}} \ . \tag{4.15}$$

Since (4.15) contains $e^{iN\omega}$, $I_q(\omega)$ has the period of $2\pi/N$. Therefore $I_q(\omega)$ has a train of peaks, which is shown in Fig. 4. These peaks become sharp as q decreases further below q_c. Furthermore, from (4.2) $a+\beta \to 1$ as $q \to q_c$, so we note that the coefficient of $e^{iN\omega}$ term decreases as $q \to q_c$. In other words, as q is increased, the peaks disappear at $q = q_c$ and $I_q(\omega)$ changes to be white-noise type for $q > q_c$.

Next we consider the envelope of $I_q(\omega)$. The extremum points $\{\omega_k\}$ of $I_q(\omega)$ are determined by

$$\frac{1-ae^{i\omega}}{1-ae^{-i\omega}} e^{iN\omega} = \frac{i\beta(1-\delta)\sin(\omega) \pm \delta(1-\cos\omega)[1+a^2-2a\cos\omega]^{1/2}}{(1-e^{-i\omega})\delta(1+a)-i\delta^2 e^{-i\omega}\sin\omega - 2ia\sin\omega} \ , \tag{4.16}$$

where $\delta = a+\beta$ and the $+(-)$ sign corresponds to the positions of the local maxima (minima) of $I_q(\omega)$. By inserting (4.16) into (4.15), the envelopes of $I_q(\omega)$ are given by

$$[I_q(\omega)]_{\text{env}} = \frac{[\beta(1-\delta)+a(1-\cos\omega)-\beta(1-\delta)(A\cos\omega + B\sin\omega)]\mu_N}{1+\delta^2-\delta(1-\cos\omega)-(1-\delta)[A(1-a\cos\omega)-B\delta\sin\omega]} \ , \tag{4.17}$$

where $A+iB$ is equal to the right-hand side of (4.16).

After a straightforward calculation for small ω, Eq. (4.17) yields

$$[I_q(\omega)]_{\text{env}} \propto \begin{cases} \omega^{-2} & \text{(upper envelope)} \\ \text{constant} & \text{(lower envelope)} \ . \end{cases} \tag{4.18}$$

On the other hand, in the limit $q \to -\infty$ we find

$$[I_q(\omega)]_{\text{env}} \propto \begin{cases} \omega^{-2} & \text{(upper envelope)} \\ \omega^2 & \text{(lower envelope)} \end{cases} \tag{4.19}$$

for small ω. Therefore the upper envelope of $I_q(\omega)$ exhibits a power-law dependence on ω with the exponent 2 independently of q. This behavior of the envelope is illustrated in Fig. 5. The solid line $\beta = 0$ (i.e., $q = -\infty$) apparently shows $[I_q(\omega)]_{\text{env}} \propto \omega^{-2}$, whereas for $\beta = 0.4$ ($q = q_c$), $I_q(\omega)$ becomes independent of ω. Upper envelopes obey power law in the low-frequency region for $q < q_c$ and the region shrinks as $q \to q_c$. For lower envelopes the ω-independent region shrinks as $q \to -\infty$ and at $q \to -\infty$ $I_q(\omega)$ obeys power law in a wide ω region.

The above qualitative change between two regions $q < q_c$ and $q > q_c$ is an eminent characteristic of order-q power spectra associated with the q-phase transition. Changing the value of q, one can thus single out various statistical characteristics (even including a pure burst phase). In the previous paper we obtained the ω^{-1} law for the order-q power spectrum for the tangency map whose order of tangency is 2[13]. In a type-I intermittency map, the order-q power spectrum for the symbolized

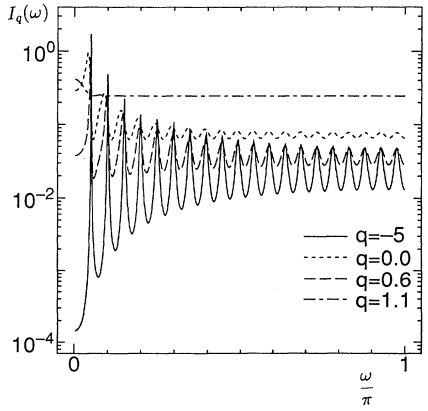

FIG. 4. The order-q power spectrum $I_q(\omega)$ of SC for several q's for $m = 20$. For large q, it is independent of q. On the other hand, for small q, $I_q(\omega)$ shows a train of peaks.

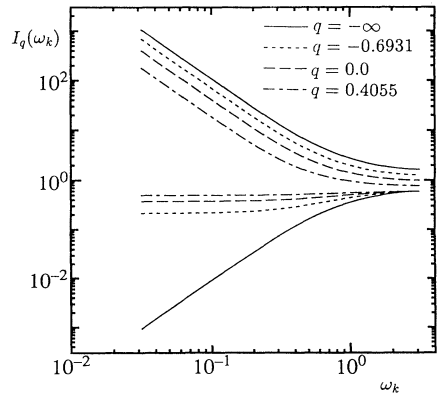

FIG. 5. The envelope of $I_q(\omega)$ in the case of SC for $\beta = 0.0$ ($q = -\infty$), 0.1 ($q = -0.6931$), 0.2 ($q = 0.0$), and 0.3 ($q = 0.4055$) in the limit $m = \infty$, i.e., $a = a_c + 0$. Solid line denotes the case of $q = -\infty$ ($\beta = 0$).

dynamics always shows a power-law form $\omega^{-\theta}$ for q smaller than a characteristic value of q, and the exponent θ depends only on the order of tangency at channel and is independent of q. We plan to discuss this dependence in a separate paper.

V. DYNAMICS OF LOCAL EXPANSION RATES

In this section we will consider the dynamics of local expansion rates from the view-point of fluctuation functions and order-q power spectrum. Fluctuation functions and the q-phase transition of LER have been discussed a in previous paper [15]. Moreover, there have been several published works on thermodynamic formalisms for local expansion rates [4,16]. In this case, the characteristic equation is written in the following way:

$$\beta^{-1}=\frac{1-\left[\frac{\alpha}{\nu}\right]^{m+1}}{\nu-\alpha}+\frac{1}{\nu^N}\frac{1-(\nu\alpha)^m}{1-\nu\alpha}\ , \tag{5.1}$$

where ν is the eigenvalue, $\alpha=a^{1-q}$, and $\beta=b^{1-q}$. Eigenvalues of H_q are also separated into two groups as in the symbolized dynamics case, which is shown in Fig. 6. The largest eigenvalue for $m\to\infty$ is found to be

$$\nu_q=\begin{cases}1 & (q\le q_c)\\ \alpha+\beta & (q\ge q_c)\ .\end{cases} \tag{5.2}$$

Since $\nu_{qc}=1$, we get $q_c=0.2728\ldots$. Now the fluctuation functions are obtained from (2.4a), (2.6a), and (2.6b) as

$$\phi(q)=\begin{cases}0 & \text{for } q\le q_c\\ \ln(\alpha+\beta) & \text{for } q\ge q_c\ ,\end{cases} \tag{5.3}$$

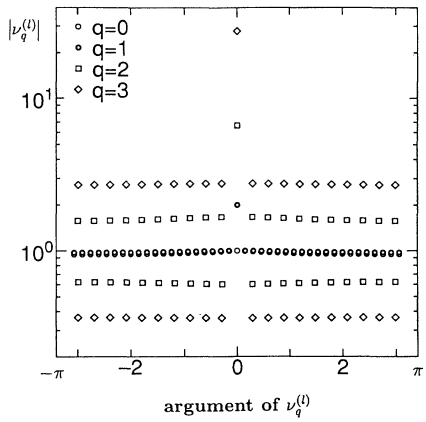

FIG. 6. Distribution of eigenvalues $\nu_q^{(l)}$ of H_q for LER. As q increases, the largest eigenvalue increases, and the radius of the circle on which other eigenvalues lie becomes large.

$$U(q)=\begin{cases}0 & \text{for } q<q_c\\ \dfrac{-(\alpha\ln a_c+\beta\ln b)}{(\alpha+\beta)} & \text{for } q>q_c\ ,\end{cases} \tag{5.4}$$

$$\chi(q)=\begin{cases}0 & \text{for } q<q_c\\ +\infty & \text{for } q=q_c\\ \dfrac{\alpha\beta(\ln a_c-\ln b)^2}{(\alpha+\beta)^2} & \text{for } q>q_c\ .\end{cases} \tag{5.5}$$

The fluctuation spectrum $\sigma(U)$ is obtained from (2.7)

$$\sigma(U)=\begin{cases}q_c U & \text{for } 0\le U\le\Delta\\ U+\dfrac{R(\ln(ae^U))+R(\ln(b^{-1}e^{-U}))}{\ln(a/b)}-\ln\ln(a/b) & \text{for}\ \Delta\le U\le U_{\max}\ ,\end{cases} \tag{5.6}$$

where $R(x)\equiv x\ln x$, $U_{\max}=-\ln b\simeq 1.6094$, and $\Delta\equiv U(q_c+0)\simeq 0.8517$. These fluctuation functions are drawn in Fig. 7. In the case of LER, the q-phase transition also occurs. However, the critical point $q_c=0.2728\ldots$ is different from that for the symbolized dynamics. The asymptotic behaviors of fluctuation functions for LER are the same as those for SC.

Furthermore, after a few calculations, the peak height $\chi_N(\hat{q})$ of $\chi_N(q)$ is found to obey

$$\chi_N(q)\propto N \tag{5.7}$$

for large N. The numerical observation shows that $\hat{q}(N)$, the peak position of $\chi_N(q)$, satisfies

$$q_c-\hat{q}\propto N^{-\eta}\ , \tag{5.8}$$

where $\eta\simeq 0.8$. Therefore one observes the phase transition at $q=q_c$ as q is changed near the bifurcation point. These fluctuation functions for finite N are shown also in Fig. 7. As shown in Ref. [17], their fluctuation functions satisfy the scaling laws for finite N.

Next, we turn to the order-q power spectrum. Equations (3.4) and (3.5) were evaluated numerically. $I_q(\omega)$ is shown in Fig. 8. As in the SC case, these spectra exhibit white-noise-type characteristics for $q>q_c$ and m trains of peaks for $q<q_c$. This transition between two regions occurs in a clear-cut way as q is changed as shown in Fig. 8. Each peak of $I_q(\omega)$ for $q<q_c$ becomes sharper as N increases. The height of peak is larger and sharper in the low frequency region. (In Fig. 8 we do not see the true height at small frequencies because the peaks are too sharp to sample with equal increment of ω.) Envelopes of $2k$th and $(2k+1)$th peaks seem to obey different power laws, which are illustrated in Fig. 9. The exponents of odd and even peaks are found to be -3.8 and -1.9, respectively. This is quite different from the SC case.

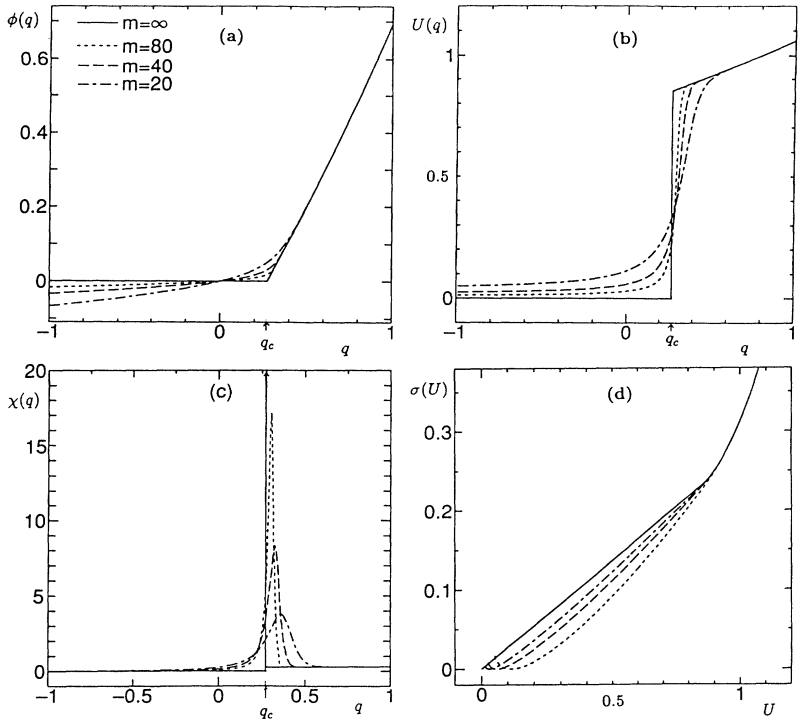

FIG. 7. Static fluctuation functions for LER of the SOM map at $a=a_c+0$ (solid lines), where $q_c=0.2728\ldots$, $\Delta\equiv U(q_c+0)\simeq 0.8517\ldots$. The fluctuation functions for finite m, i.e., for finite-number Markov partition, are also shown.

The complicated structure of $I_q(\omega)$ illustrated in Fig. 8 comes from a discontinuity of $u(x)$ at channel. As the system parameter approaches the onset of chaos, the region of channel becomes narrow. For almost all time, the orbit stays in the channel region. For $q<q_c$, we observe most dominant motion, which is laminar motion on small channel. However, if there is some discontinuity of $u(x)$ at the channel, we observe different local average $\overline{U}_n$ between reinjections before and after the channel, even though the channel becomes so small. These $\overline{U}_n$ are produced from $2m$ and m period, respectively. Therefore $I_q(\omega)$ is composed of peaks corresponding to $2m$ and m period. As a result, the shape of $I_q(\omega)$ becomes complicated. Local expansion rates are usually continuous at the channel. In this respect, the SOM map is a special example which gives a complicated structure of $I_q(\omega)$ of LER. But we must stress that this kind of $I_q(\omega)$ is ubiquitous for observation with discontinuities only in cases where the realization probability is dominant.

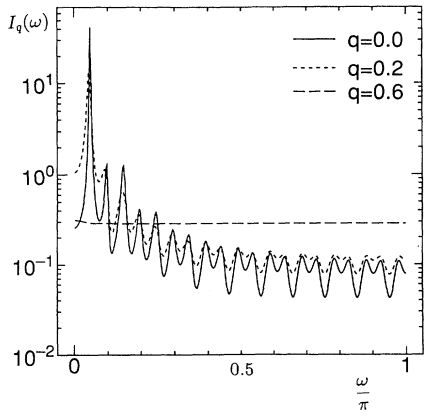

FIG. 8. $I_q(\omega)$ in the case of LER for several q's at $m=20$. One observes a qualitative change of $I_q(\omega)$ when $q=q_c$.

VI. CONCLUSION

In the present paper we analyzed the type-I intermittency phenomena using the So-Ose-Mori map whose order of tangency is unity. This was carried out by observing how the fluctuation characteristics of the symbolized dynamics and the local expansion rate dynamics change as the system approaches the intermittency transition point. Their statistical properties were investigated from the standpoint of the fluctuation functions $\phi(q)$, $U(q)$, $\sigma(U)$, etc., and the order-q power spectrum $I_q(\omega)$, which are, respectively, relevant to the overall (long-time) statistics of temporal fluctuations and the explicit temporal correlations. A distinctive feature of the present approach is that we can clearly single out the two different characteristics of motion, laminar phase and burst, by introducing an intensive variable q. By changing the value of q, one can describe many statistics which are due to coexistence of laminar phase and burst.

It was shown that near the transition point of the external control parameter, the relevant functions for the fluctuation spectrum exhibit nonanalytical behaviors at certain value of q as the parameter q is changed. This phenomenon is known as the q-phase transition. We have shown that such transitions in the q space are observed both for SC and for LER, though their transition points are different from each other. Below the transition point $q_c(>0)$, the statistics are dominantly determined

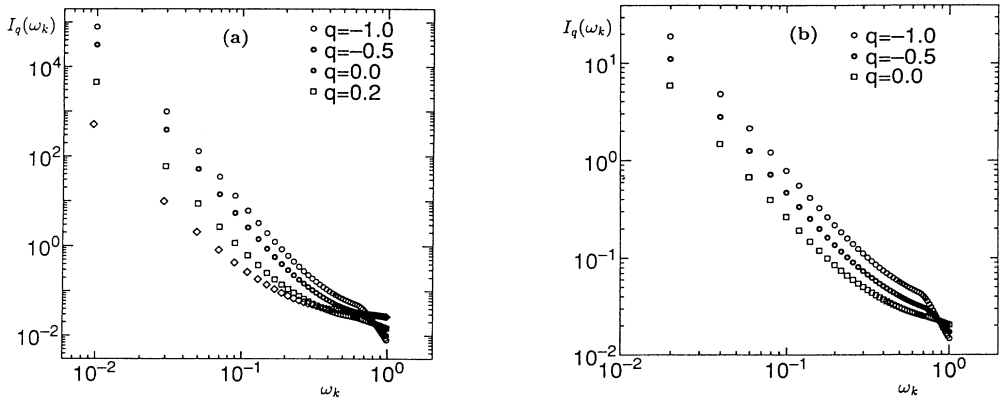

FIG. 9. The envelope of $I_q(\omega)$ in case of LER for several q: (a) for odd peaks and (b) for even peaks.

by laminar phase and, above q_c, by burst phase. At the transition point q_c, the role of these two distinctive motion interchanges as q is changed. This is the reason for the existence of such q-phase transition.

In the present paper we found several scaling behaviors of relevant functions near the critical point. Let us give a comment on the asymptotic form (4.8). Recently Mori pointed out that the asymptotic form (4.8) could be replaced as

$$q_c - \hat{q} \propto N^{-1}\ln(N) \tag{6.1}$$

in the critical regions [18]. This is obtained by analyzing

$$q - q_c \simeq \frac{\nu-1}{1-a} - e^{-N(\nu-1)}, \tag{6.2}$$

which is derived by evaluating (4.1) for large N and $\nu-1 \ll 1$. The exponent η from (6.1) is $1-0$ and is different from 0.8 numerically obtained. The law (6.1) is valid for sufficiently large $N[=O(10^6)]$. The value $\eta=0.8$ is obtained up to $N=O(10^2)$. For such N values the logarithmic factor cannot be neglected and tends to decrease the exponent 1. In this sense our numerical result 0.8 is not incompatible with (6.1). Furthermore, by making use of (6.2) one can derive the analytical expression for the fluctuation functions.

As is well known, the hallmark of the type-I intermittency is the anomalous temporal correlations, i.e., power law of the power spectral density. In the present paper we have calculated the order-q power spectra $I_q(\omega)$ for SC and LER. Both these power spectra also undergo the transition at q_c which is the same as that for the fluctuation functions. In the limit of the intermittency transition of the control parameter, the local maximum of the order-q power spectrum drastically changes as q is changed, i.e., for $q < q_c$ (laminar phase) it shows a power law ω^{-2}, the exponent 2 being independent of q, while for $q > q_c$ (burst) it is independent of ω (white noise). The power spectrum of the type-I intermittency is believed to show a power law, but in addition we also found white-noise characteristics. This is, as is expected, due to the fact that we succeeded in taking out the burst dynamics separately by choosing the parameter value of q.

In a previous paper, we found ω^{-1} for intermittency map whose order of tangency of channel is 2. The power law of the order-q power spectrum, with the q-independent exponent, is a distinctive feature of type-I intermittency. Such a simple law for the order-q power spectrum is reduced to a "simple" structure for the temporal behaviors of intermittency. In fact we have a system with the q-dependent exponent as reported in Ref. [19]. Recently Fukushima and Yamada carried out the experiment on the breakdown of the synchronization of the chaotic oscillators in an electronic circuit and observed intermittent characteristics. This intermittency is quite different from the three well-known types of intermittency. They analyzed intermittent signals with the order-q power spectrum, and found that it exhibit a power law $\omega^{-\theta(q)}$, where the exponent θ depends monotonously on q. This tells us that, contrary to the type-I intermittency, the intermittency associated with the desynchronization of chaos contains more complex temporal evolution.

ACKNOWLEDGMENTS

We wish to thank our chaos group at Kyushi University for stimulating and useful discussions. Two of the authors (T.K. and W.J.) are grateful to the Japan Society for the Promotion of Science. W.J. is also greatly indebted to the Alexander von Humboldt Stiftung (Germany) for financial support. Finally, we would like to express our thanks to the Communications Research Laboratory for their financial support.

*Present address: Communications Research Laboratory, Nukui-Kitamachi 4-2-1, Koganei 184, Japan. Electronic address: tkoba@cc.crl.go.jp

†Present address: Theoretische Festkörperphysik, Technische Hochschule Darmstadt, Hochschulestrasse 8, D-6100 Darmstadt, Federal Republic of Germany.

[1] J. Guckenheimer and P. Holmes, *Nonlinear Oscillations, Dynamical Systems, and Bifurcations of Vector Fields* (Springer-Verlag, New York, 1983); P. Berge, Y. Pomeau and C. Vidal, *Order Within Chaos* (Wiley, New York, 1984); H. G. Schuster, *Deterministic Chaos* (VCH, Weinheim, 1988).

[2] H. Fujisaka, Prog. Theor. Phys. **70**, 1264 (1983); H. Fujisaka and M. Inoue, *ibid.* **77**, 1334 (1987).
[3] T. C. Halsey, M. H. Jensen, L. P. Kadanoff, I. Procaccia, and P. I. Schraiman, Phys. Rev. A **33**, 1141 (1986).
[4] Y. Takahashi and Y. Oono, Prog. Theor. Phys. **71**, 851 (1984); P. Szepfalusy and T. Tel, Phys. Rev. A **34**, 2520 (1986); T. Morita, H. Hata, H. Mori, T. Horita, and K. Tomita, Prog. Theor. Phys. **79**, 296 (1988); T. Bohr and D. Rand, Physica D **25**, 387 (1989); S. Vaienti, J. Stat. Phys. **56**, 403 (1989).
[5] J. P. Eckmann and I. Procaccia, Phys. Rev. A **34**, 659 (1986); M. Sano, S. Sato, and Y. Sawada, Prog. Theor. Phys. **76**, 945 (1986); D. Bessis, G. Paladin, G. Turchetti, and S. Vaienti, J. Stat. Phys. **51**, 109 (1988); P. Grassberger, R. Badii, and A. Politi, *ibid.* **51**, 135 (1988).
[6] G. Paladin and A. Vulpiani, Phys. Rep. **156**, 147 (1987).
[7] Ya. G. Sinai, Usp. Math. Nauk **27**, 21 (1972); R. Bowen, in *Equilibrium States and Ergodic Theory of Anosov Diffeomorphisms,* edited by A. Dold and B. Eckmann, Lecture Notes in Mathematics Vol. 470 (Springer-Verlag, Berlin, 1975); D. Ruelle, Am. J. Math. **98**, 619 (1976); D. Ruelle, *Encyclopedia of Mathematics and its Applications, Vol. 5 Thermodynamic Formalism* (Addison-Wesley, Reading, MA, 1978).
[8] R. S. Ellis, *Entropy, Large Deviations, and Statistical Mechanics* (Springer-Verlag, New York, 1985).
[9] H. Mori, B. C. So, and T. Ose, Prog. Theor. Phys. **66**, 1266 (1981).
[10] H. Mori, H. Hata, T. Horita, and T. Kobayashi, Prog. Theor. Phys. Suppl. No. **99**, 1 (1989).
[11] H. Fujisaka and H. Shibata, Prog. Theor. Phys. **85**, 187 (1991).
[12] H. Fujisaka and M. Inoue, Prog. Theor. Phys. **78**, 268 (1987).
[13] W. Just and H. Fujisaka, Physica D (to be published).
[14] H. Shibata, S. Ando, and H. Fujisaka, Phys. Rev. A **45**, 7049 (1992).
[15] N. Mori, T. Kobayashi, H. Hata, T. Morita, T. Horita, and H. Mori, Prog. Theor. Phys. **81**, 60 (1989).
[16] X. J. Wang, Phys. Rev. A **40**, 6647 (1989); K. Honda, S. Sato, and H. Kodama, *ibid.* **43**, 2669 (1991).
[17] T. Kobayashi, N. Mori, H. Hata, T. Horita, T. Yoshida, and H. Mori, Prog. Theor. Phys. **82**, 1 (1989).
[18] N. Mori (private communication).
[19] K. Fukushima and T. Yamada (unpublished).